# Consistent Boundary Conditions for Multicomponent Real Gas Mixtures Based on Characteristic Waves

Nora Okong'o, Josette Bellan, and Kenneth Harstad

*Jet Propulsion Laboratory, California Institute of Technology, 4800 Oak Grove Drive, MS125-109, Pasadena, CA 91109-8099*

*Telephone:( 818) 354-6959, FAX: (818) 393-5011*

E-mail: josette.bellan@jpl.nasa.gov

Previously developed characteristic-wave-based boundary conditions for multicomponent perfect gas mixtures are here extended to account for real gases. Following the general methodology, the characteristic boundary conditions are derived from the wave decomposition of the inviscid Euler equations, and the wave amplitude variations are determined from the prescribed boundary conditions on the flow variables in conjunction with a general real gas equation of state. The formulation is tested on the propagation of acoustic waves which are shown to exit the computational domain with minimal reflection at a subsonic non-reflecting outflow boundary. The results from this formulation are compared with those of a simplistic substitution of the real gas thermodynamic properties into previously derived, perfect gas characteristic relations, and it is shown that the simplistic substitution is deficient, particularly for situations with species sources (representing mass emission and/or chemical reactions) in the computational domain.

Key words: partial differential equations, fluid mechanics, classical thermodynamics and heat transfer.

## CONTENTS



## 1. INTRODUCTION

Boundary conditions for fluid dynamic equations play a crucial role in determining the character of the solution. Since most fluid dynamic problems of practical interest are complex, a solution to the set of differential equations and boundary conditions is usually found numerically rather than analytically. For these types of solutions Poinsot and Lele [1] distinguish between physical and numerical boundary

conditions. The physical boundary conditions are those that are intrinsically imposed by the problem to be solved and are associated with the differential equations. The numerical boundary conditions are associated with the difference implementation of the differential equations and can be considered as compatibility relations that must be added to the physical boundary conditions to palliate the uncertainty in the variables that are not specified by the physical boundary conditions. Indeed, for some types of physical problems described by the Euler or Navier-Stokes (NS) equations, the number of necessary and sufficient boundary conditions is smaller than the number of primitive variables [2], [1], and the issue of the specification of the remaining number of variables introduces the concept of numerical boundary conditions. As Poinsot and Lele [1] note, these numerical boundary conditions must satisfy the differential equations and also must prevent the introduction of spurious numerical effects such as wave reflections from the boundaries of the computational domain.

Boundary conditions derived from characteristic wave analysis were presented by Kreiss [3], Engquist and Majda [4], Higdon [5], Thompson [6], Poinsot and Lele [1] and Baum et al. [7]. Although this type of analysis is consistent with the Euler equations, it does not seem applicable to the NS equations which are not hyperbolic. The essential idea of using a characteristic wave analysis for the NS equations is discussed by Dutt [2] and is based on the fact that at high Reynolds number, Re, the NS equations may be considered as an incompletely elliptic perturbation of the Euler equations. Gustafsson and Sundström [8] note that while for finite Re the NS equations cannot be classified as hyperbolic, elliptic or parabolic, for $\mathrm{Re} \to \infty$ the NS equations constitute a quasi-linear hyperbolic system. Therefore, at these

conditions the essence of the NS equations may be considered to be hyperbolic, with the diffusive terms providing only 'corrections' to their hyperbolic behavior. This crucial observation allowed Poinsot and Lele [1] to use Thompson's [6] derivation of numerical boundary conditions for hyperbolic systems to derive a similar set for the NS equations. When implemented for a variety of example problems, these numerical boundary conditions proved robust and yielded solutions in agreement with the expected physics of the problem. More recently, Baum et al. [7] extended the work of Poinsot and Lele [1] to multicomponent reactive flow problems where the new issue is that of the source terms in the mass fraction and energy equations. Although not explicitly stated, this extension implicitly assumed that the mass fractions and energy equations may also be an incompletely elliptic perturbation of the Euler-type equations. This implication is correct since in the classical, low pressure equations the molar and heat fluxes are proportional to $(Sc\,\mathrm{Re})^{-1}$ and $(\mathrm{Pr}\,\mathrm{Re})^{-1}$, respectively, where $Sc$ is the Schmidt number and Pr is the Prandtl number. These studies were all performed for fluids obeying the perfect gas law.

However, there are many practical applications where the fluid is not a perfect gas. Such situations occur in high pressure reactive flows typical of rocket engines, Diesel engines or gas turbine engines, as well as in fluid flowing in pipes laid on the ocean floor. The importance of real gas equations of state (EOSs) was highlighted by Shyue [9] in his development of the algorithm for compressible multicomponent liquid-gas flow using the van der Waals EOS. The new algorithm was built on a previous interface-capturing approach and focussed on accurate wave tracking resolution, including shock tracking.

The present work is devoted to the derivation of accurate and consistent boundary conditions for reactive flows where the fluid is a real gas. Section 2 is first devoted to new aspects of the conservation equations that may be important for real gases, and then to the derivation of the boundary conditions. This derivation follows the method of Thompson [6], Poinsot and Lele [1] and Baum et al. [7] whereby a local one-dimensional inviscid (LODI) set of equations, described at the boundary in characteristic form, embodies the essential behavior at the boundary. The wave amplitude variation in the characteristic wave formulation is then consistently computed to satisfy the desired boundary conditions for a general real gas EOS, and the viscous conditions are separately applied as in Poinsot and Lele [1]. In Section 3 we discuss the generic implementation of these boundary conditions for typical problems encountered in fluid dynamics, and in Section 4 we test the derived boundary conditions for three specific problems involving propagation of acoustic waves. We compare the results of these calculations with those of similar calculations where the results of Baum et al. [7] are simplistically used by replacing in their final results the perfect gas thermodynamic quantities with equivalent real gas quantities, and we show that the simplistic approach leads to numerical problems and inaccuracies. Finally, we summarize this work and offer further comments in the Conclusion section.

## 2. GENERAL EQUATIONS

Harstad and Bellan [10], [11], [12] have derived the multicomponent conservation equations for real gases, non ideal mixtures. These equations have the typical form of the NS equations augmented by the species and energy equations, and by

the EOS, with the exception that the diffusive terms in the species and energy equations now contain additional terms. In the species and energy equations, the respective Fick mass diffusion and Fourier heat diffusion terms are now respectively complemented by the Soret and Dufour terms representing the thermal diffusion contribution. These conservation equations are

$$\frac{\partial \rho}{\partial t} + \frac{\partial \left(\rho u_j\right)}{\partial x_j} = 0, \tag{1}$$

$$\frac{\partial \left(\rho u_i\right)}{\partial t} + \frac{\partial \left(\rho u_i u_j + p\delta_{ij}\right)}{\partial x_j} = \frac{\partial \tau_{ij}}{\partial x_j}, \tag{2}$$

$$\frac{\partial \left(\rho E_T\right)}{\partial t} + \frac{\partial \left[\left(\rho E_T + p\right) u_j\right]}{\partial x_j} = -\frac{\partial q_{IKj}}{\partial x_j} + \frac{\partial (\tau_{ij} u_i)}{\partial x_j}, \tag{3}$$

$$\frac{\partial \left(\rho Y_\alpha\right)}{\partial t} + \frac{\partial \left(\rho Y_\alpha u_j\right)}{\partial x_j} = -\frac{\partial J_{\alpha j}}{\partial x_j}, \tag{4}$$

where $t$ is the time, $x_j$ is the $j$th coordinate, $\rho$ is the mass density, $u_j$ is the $j$th velocity component, $T$ is the temperature, $Y_\alpha$ is the mass fraction of species $\alpha$ (for $N$ species $\sum_{\beta=1}^{N} Y_\beta = 1$), $p$ is the pressure and $E_T = E + \frac{1}{2} u_i u_i$ is the total energy (internal energy, $E$, plus kinetic energy). Additionally, $\tau_{ij}$ is the Newtonian viscous stress tensor

$$\tau_{ij} = \mu \left[ \frac{\partial u_i}{\partial x_j} + \frac{\partial u_j}{\partial x_i} - \frac{2}{3} \frac{\partial u_k}{\partial x_k} \delta_{ij} \right], \tag{5}$$

where $\mu$ is the mixture viscosity which is in general a function of the thermodynamic state variables, $J_\alpha$ is the molar flux and $q_{IK}$ is the Irwing-Kirkwood (subscript $IK$) form of the heat flux [13]. The Einstein summation convention (summation over repeated indices) is used for $i$ and $j$, but not over Greek indices $\alpha$ and $\beta$.

For example, in this general situation which includes thermal diffusion effects, the molar and heat fluxes [14] for a binary mixture are given by

$$J_{1j} = -\left[J'_{1j} + (\alpha_{IK} - \alpha_h) Y_1 Y_2 \frac{\rho D}{T} \frac{\partial T}{\partial x_j}\right], \tag{6}$$

$$q_{IKj} = -\lambda'_{IK} \frac{\partial T}{\partial x_j} + \alpha_{IK} R_u T \frac{m}{m_1 m_2} J'_{1j}, \tag{7}$$

$$J'_{1j} = \rho D \left[\alpha_D \frac{\partial Y_1}{\partial x_j} + \frac{Y_1 Y_2}{R_u T} \frac{m_1 m_2}{m} \left(\frac{v_1}{m_1} - \frac{v_2}{m_2}\right) \frac{\partial p}{\partial x_j}\right], \tag{8}$$

$$\alpha_h = \frac{1}{R_u T} \frac{m_1 m_2}{m} \left(\frac{h_1}{m_1} - \frac{h_2}{m_2}\right), \tag{9}$$

where $D$ is the mass diffusivity, $m_\alpha$ is the species molar weight, $m = \sum_{\alpha=1}^{N} m_\alpha X_\alpha$ is the mixture molar weight, $R_u$ is the universal gas constant, $\lambda'_{IK}$ is a thermal conductivity (see below), $\alpha_D$ is the mass diffusion factor calculated from the fugacity, $\varphi_\alpha$, as

$$\alpha_D = 1 + X_\alpha \frac{\partial \ln(\varphi_\alpha)}{\partial X_\alpha}, \tag{10}$$

and $\alpha_{IK}$ is the IK thermal diffusion factor [11], [12] corresponding to the IK form of the heat flux. The quantities

$$v_\alpha = (\partial v/\partial X_\alpha)_{T,p,X_{\beta(\beta\neq\alpha)}} \quad \text{and} \quad h_\alpha = (\partial h/\partial X_\alpha)_{T,p,X_{\beta(\beta\neq\alpha)}} \tag{11}$$

are the partial molar volume and the partial molar enthalpy, respectively, $v$ and $h$ being the molar volume and molar enthalpy, respectively. Furthermore, the molar volume $v$ is related to the density by $v = m/\rho$, and $X_\alpha = mY_\alpha/m_\alpha$ is the species molar fraction. The thermal conductivity $\lambda'_{IK}$ is defined in [11] and [12] from the transport matrix. It can be shown that $\lambda'_{IK}$ does not correspond to the kinetic theory (subscript $KT$ ) definition of the thermal conductivity in that $\lim_{p\to 0} \lambda'_{IK} \neq \lambda_{KT}$ but it is related to the thermal conductivity, $\lambda$, through

$$\lambda'_{IK} = \lambda + X_1 X_2 \; \alpha_{IK} \; (\alpha_{IK} - \alpha_h) R_u \rho D/m, \tag{12}$$

where $\lim_{p\to 0} \lambda = \lambda_{KT}$ as discussed in [11] and [12]. Although currently there is no information as to the functional form of $\alpha_{IK}$ with respect to the primary variables $(p, T, Y_i)$ and/or its magnitude, Harstad and Bellan [11], [12] have determined its approximate value for the heptane-nitrogen pair from comparisons of numerical predictions with a partial set of data; once this coefficient was determined, the remaining part of the data set was used to validate the model.

Therefore, the general form of the flux matrix is

$$J = A_J \frac{\partial Y_1}{\partial x} + B_J \frac{\partial T}{\partial x} + C_J \frac{\partial p}{\partial x} \tag{13}$$

$$q = A_q \frac{\partial T}{\partial x} + C_q \frac{\partial Y_1}{\partial x} + B_q \frac{\partial p}{\partial x} \tag{14}$$

where the coefficients of this matrix can be identified from direct comparisons with Eqs. 6-9. Clearly, it is difficult a priori to state what is the essential character of these equations: parabolic, elliptic or hyperbolic. Since the present boundary conditions derivation is intended to be valid at higher than atmospheric pressures, and since the Soret and Dufour contributions are known to become progressively more important with increasing pressure [15], the question arises as to whether Dutt's [2] conditions regarding the form of the equations that may be treated with the characteristic wave approach is still satisfied. It is outside the scope of this work to prove that the condition of the incomplete elliptic perturbation is here valid for the mass fractions and energy equations; instead, we base our inference on a comparison with the familiar set of equations discussed by Baum et al. [7]. If we can show that there is a set of variables for which the more general equations including Soret and Dufour effects assume a form similar to the diffusion equations based on the Fick and Fourier diffusive fluxes, then we will assume that the method of Baum et al. [7] remains valid.

An analytical diagonalization of the species and energy equations operators under the quasi-steady, boundary layer assumptions yields eigenvalues of the transport matrix [16], which for a binary mixture are an effective mass diffusivity, $D_{eff}$, and a thermal conductivity, $\lambda_{eff}$, quantifying departures from $D$ and $\lambda$

$$D_{eff} = \alpha_D D(1 - X_1 X_2 \alpha_{BK}^2 R_u n D\varsigma) \tag{15}$$

$$\lambda_{eff} = \lambda + X_1 X_2 \alpha_{BK}^2 R_u n D (1 + n D \alpha_D C_p \varsigma) \tag{16}$$

where $\varsigma$ is the positive root of an algebraic equation, $n = \rho/m$ is the molar density, and $C_p$ is the molar heat capacity at constant pressure. In Eqs. 15 and 16 $\alpha_{BK}$ is the Bearman-Kirkwood (subscript $BK$) thermal diffusion factor corresponding to the BK form of the heat flux ([13]). It can be shown that $\lim_{p\to 0} \alpha_{IK} \neq \alpha_{KT}$ and $\lim_{p\to 0} \alpha_{BK} = \alpha_{KT}$, and that [12]

$$\alpha_{BK} = \alpha_{IK} - \alpha_h. \tag{17}$$

$\alpha_{IK}$ and $\alpha_{BK}$ are the new transport coefficients that are introduced by the Soret (in the molar fluxes) and the Dufour (in the heat flux) terms of the transport matrix, and are characteristic of the particular species pairs under consideration. Since $\alpha_h$ is a thermodynamic function, it is sufficient to know either $\alpha_{IK}$ or $\alpha_{BK}$ to have the other thermal diffusion factor determined. The values of $\alpha_{IK}$ and $\alpha_{BK}$ will be discussed in Section 4.

Since the second term in the right hand side of Eq. 15 and the third term in the right hand side of Eq. 16 are both positive, it is apparent that the mass diffusivity diminishes whereas the thermal conductivity is enhanced as thermal diffusion effects become important. Both effective coefficients are indeed positive defined (as they physically should be), indicating that the set of new equations is of the type discussed by Baum et al. [7], and that the concepts of Dutt [2] may still apply. The same analysis can be extended to $N$ component mixtures with similar results,

yielding $N$ effective mass diffusivities. However, it is immediately clear that the ellipticity of the system of equations is not determined by the effective diffusivities which are always reduced compared to ideal mixtures ($\alpha_D = 1$) atmospheric conditions ($\alpha_{BK} \ll 1$) situations, because for non-ideal mixtures $\alpha_D < 1$ and if thermal diffusion effects are important one may have $X_1 X_2 \alpha_{BK}^2 R_u n D\varsigma$ comparable to unity. What truly determines the level of ellipticity of the system is $\lambda_{eff}$ which may possibly reach large values compared to $\lambda$. Calculations performed with this model [12] for heptane-nitrogen in the present range of $(p, T)$ (see Section 4) yielded $\lambda_{eff} = O(\lambda)$. Based on this circumstantial evidence it is still relevant to proceed with the derivation of relations based on characteristic lines in order to analyze the fate of waves crossing the boundary of a computational domain. However, we note that because of the enhanced value of $\lambda$, the ellipticity of the system of equations does increase with increasing pressure, and depending on the values of the thermal diffusion factors the essentially hyperbolic behavior of the system may be lost.

As in Poinsot and Lele [1] and Baum et al. [7], we start by analyzing the Euler equations, which contain the needed characteristic behavior at the boundaries. Whereas in principle the entire enlarged Navier-Stokes equations should be analyzed, in fact the Euler equations alone provide the characteristic behavior of the solution and therefore they are analyzed hereafter.

### 2.1. Euler Equations

The conservative form of the Euler equations augmented by the species and energy equations is

$$\frac{\partial \rho}{\partial t} + \frac{\partial (\rho u_j)}{\partial x_j} = 0, \tag{18}$$

$$\frac{\partial (\rho u_i)}{\partial t} + \frac{\partial (\rho u_i u_j)}{\partial x_j} + \frac{\partial p}{\partial x_i} = 0, \tag{19}$$

$$\frac{\partial (\rho E_T)}{\partial t} + \frac{\partial}{\partial x_j} \left[ (\rho E_T + p) \, u_j \right] = 0, \tag{20}$$

$$\frac{\partial (\rho Y_\alpha)}{\partial t} + \frac{\partial (\rho Y_\alpha u_j)}{\partial x_j} = 0, \ \alpha = 1, N \tag{21}$$

$$E_T = \tfrac{1}{2} u_i u_i + E, \ \sum_{\alpha=1}^{N} Y_\alpha = 1 \tag{22}$$

where $E_T$ is the total energy per unit mass. This is a system of $N + 5$ differential equations in the three-dimensional case.

The pressure is given by an EOS, a state being uniquely specified by the internal energy $E$, the density and the mass fractions

$$p = p(\rho, E, Y_1, \cdots Y_N). \tag{23}$$

To perform the wave decomposition, it is more convenient to work with the Euler equations in primitive form:

$$\frac{\partial \rho}{\partial t} + u_j \frac{\partial \rho}{\partial x_j} + \rho \frac{\partial u_j}{\partial x_j} = 0, \tag{24}$$

$$\frac{\partial u_i}{\partial t} + u_j \frac{\partial u_i}{\partial x_j} + \frac{1}{\rho} \frac{\partial p}{\partial x_i} = 0, \tag{25}$$

$$\frac{\partial p}{\partial t} + u_j \frac{\partial p}{\partial x_j} + \rho c^2 \frac{\partial u_j}{\partial x_j} = 0, \tag{26}$$

$$\frac{\partial Y_\alpha}{\partial t} + u_j \frac{\partial Y_\alpha}{\partial x_j} = 0, \tag{27}$$

where the speed of sound, $c$, is given by

$$c^2 = \left(\frac{\partial p}{\partial \rho}\right)_{E,Y_\alpha} + \frac{p}{\rho^2}\left(\frac{\partial p}{\partial E}\right)_{\rho,Y_\alpha}. \tag{28}$$

(for brevity, the subscript $Y_\alpha$ on a derivative denotes that all the mass fractions are held constant). We chose here to develop the characteristic wave relationships based on the pressure rather than on the temperature because waves are directly related to $p$ rather than $T$, making the former variable the prime choice. We present in Appendix A an equivalent derivation based on $T$, similar to that of Baum et al. [7].

The pressure equation has been derived from the internal energy equation

$$\frac{\partial E}{\partial t} + \frac{p}{\rho}\frac{\partial u_j}{\partial x_j} + u_j \frac{\partial E}{\partial x_j} = 0, \tag{29}$$

by substituting

$$\frac{\partial E}{\partial x_j} = \left(\frac{\partial E}{\partial \rho}\right)_{p,Y_\alpha} \frac{\partial \rho}{\partial x_j} + \left(\frac{\partial E}{\partial p}\right)_{\rho,Y_\alpha} \frac{\partial p}{\partial x_j} + \sum_\beta \left(\frac{\partial E}{\partial Y_\beta}\right)_{\substack{\rho,p,Y_\alpha \\ \alpha\neq\beta}} \frac{\partial Y_\beta}{\partial x_j}, \tag{30}$$

and a similar expression for $\partial E/\partial t$ into Eq. 29. The internal energy derivatives appearing in Eq. 30 can be computed from the EOS, as described below.

### *2.1.1. Real Gas Relations*

The EOS, assumed here to have the most general form $p = p(T, v, Y_1, \cdots, Y_N)$, is the relationship from which $c$ as well as $\left(\frac{\partial E}{\partial \rho}\right)_{p,Y_\alpha}$, $\left(\frac{\partial E}{\partial p}\right)_{\rho,Y_\alpha}$ and $\left(\frac{\partial E}{\partial Y_\beta}\right)_{\substack{\rho,p,Y_\alpha \\ \alpha\neq\beta}}$ can all be calculated. From the EOS we can calculate the isentropic speed of sound

$$a_s^2 = \frac{1}{\rho \kappa_s}, \tag{31}$$

where $\kappa_s$ is the isentropic compressibility, which is related to the isothermal compressibility $\kappa_T$

$$\kappa_T = -\frac{1}{v\left(\partial p/\partial v\right)_{T,Y_\alpha}} \tag{32}$$

by

$$\kappa_s = \kappa_T - vT\alpha_v^2/C_p, \tag{33}$$

where

$$\alpha_v = \frac{1}{v}\left(\frac{\partial v}{\partial T}\right)_{p,Y_\alpha} = -\frac{(\partial p/\partial T)_{v,Y_\alpha}}{v\,(\partial p/\partial v)_{T,Y_\alpha}} \tag{34}$$

and $C_p$ is the molar heat capacity at constant pressure

$$C_p = \left(\frac{\partial h}{\partial T}\right)_{p,Y_\alpha} = m\left(\frac{\partial H}{\partial T}\right)_{p,Y_\alpha}, \tag{35}$$

with $H$ being the enthalpy per unit mass and $h$ being the enthalpy per mole, $h = mH$

$$H = E + \frac{p}{\rho} = E + \frac{pv}{m}. \tag{36}$$

The molar heat capacity at constant volume is

$$C_v = m\left(\frac{\partial E}{\partial T}\right)_{v,Y_\alpha} = C_p - \frac{T\alpha_v^2 v}{\kappa_T}. \tag{37}$$

In terms of the partial molar quantities, the enthalpy and molar volume are written as

$$H = \sum_{\alpha=1}^{N} h_\alpha X_\alpha / m = \sum_{\alpha=1}^{N} (h_\alpha / m_\alpha)\, Y_\alpha \; ; \qquad v = \sum_{\alpha=1}^{N} X_\alpha v_\alpha = \sum_{\alpha=1}^{N} (m v_\alpha / m_\alpha)\, Y_\alpha, \tag{38}$$

where the partial molar quantities were defined in Eq. 11. From the above thermodynamic relationships one may now calculate the desired internal energy derivatives

$$\left(\frac{\partial E}{\partial \rho}\right)_{p,Y_\alpha} = \frac{1}{\rho}\left[\frac{p}{\rho} - \frac{C_p}{m\alpha_v}\right], \tag{39}$$

$$\left(\frac{\partial E}{\partial p}\right)_{\rho,Y_\alpha} = \frac{C_p \kappa_s}{m\alpha_v} = \frac{C_p}{m\alpha_v}\frac{1}{\rho c^2}, \tag{40}$$

$$\left(\frac{\partial E}{\partial Y_\alpha}\right)_{\substack{\rho,p,Y_\beta \\ \beta\neq\alpha}} = \frac{h_\alpha}{m_\alpha} - \frac{\rho C_p}{m\alpha_v}\frac{v_\alpha}{m_\alpha}, \tag{41}$$

and one can now observe that the speed of sound is in fact the isentropic speed of sound

$$c^2 = \frac{1}{\rho \kappa_s} = a_s^2. \tag{42}$$

*2.1.2. Perfect Gas Relations*

In the perfect gas case, the EOS is

$$p = \rho R T = \frac{R_u T}{v}, \tag{43}$$

and the familiar relationships are recovered

$$h_\alpha = C_{p,\alpha} T, \tag{44}$$

$$v_\alpha = v, \tag{45}$$

$$\alpha_v = \frac{1}{v}\left(\frac{\partial v}{\partial T}\right)_{p,Y\alpha} = \frac{1}{T}, \tag{46}$$

$$\kappa_T = -\frac{1}{v\,(\partial p/\partial v)_{T,Y_\alpha}} = \frac{1}{p}, \tag{47}$$

$$\kappa_s = \kappa_T - vT\alpha_v^2/C_p = \frac{1}{\gamma p}, \tag{48}$$

where $\gamma = C_p/C_v$

$$C_v = C_p - \frac{T\alpha_v^2 v}{\kappa_T} = C_p - R_u, \tag{49}$$

$$c^2 = \frac{1}{\rho\kappa_s} = \frac{\gamma p}{\rho}.$$

The internal energy is

$$E = \frac{C_v}{m}T = \frac{p}{\rho}\frac{1}{(\gamma - 1)}, \tag{50}$$

and therefore the internal energy derivatives are:

$$\left(\frac{\partial E}{\partial \rho}\right)_{p,Y_\alpha} = -\frac{p}{\rho^2}\frac{1}{(\gamma-1)}, \tag{51}$$

$$\left(\frac{\partial E}{\partial p}\right)_{\rho,Y_\alpha} = \frac{1}{\rho}\frac{1}{(\gamma-1)}, \tag{52}$$

$$\left(\frac{\partial E}{\partial Y_\alpha}\right)_{\substack{\rho,p,Y_\beta \\ \beta\neq\alpha}} = \frac{(C_{p,\alpha}-C_p)\,T}{m_\alpha}. \tag{53}$$

We note at this point that since Poinsot and Lele [1] define $\gamma$ through Eq. 50, it is tempting to simply translate their perfect gas wave decomposition relationships, wave amplitude variations and ensuing results to real gases by replacing $\gamma-1$ with $[\kappa_s(p+\rho E)]^{-1}$. This equality is obtained from a consistency condition with the conservation equations by equating $c^2$ calculated according to Eq. 42 with $[p+\rho E(\gamma-1)]/\rho$. We call this a 'simplistic approach' in contrast with the fundamental approach taken below, and show in Section 4 that this simplistic approach does not capture the complex nature of real gas behavior.

### 2.2. Euler Equations Wave Amplitude Variations

Following the procedure introduced by Thompson [6] and elaborated by Poinsot and Lele [1] and by Baum et al. [7], the wave decomposition is performed for generic equations

$$\frac{\partial \phi}{\partial t} + \mathbf{A}^j \cdot \frac{\partial \phi}{\partial x_j} = 0, \tag{54}$$

where $\phi$ is the vector of dependent variables

$$\phi = \left\{ \rho,\ u_1,\ u_2,\ u_3,\ p,\ Y_1\ \cdots\ Y_N \right\}^T, \tag{55}$$

and $\mathbf{A}^j$ are matrices:

$$\mathbf{A}^j = \begin{bmatrix} u_j & \rho\delta_{1j} & \rho\delta_{2j} & \rho\delta_{3j} & 0 & 0 & \dots & 0 \\ 0 & u_j & 0 & 0 & \frac{1}{\rho}\delta_{1j} & 0 & \dots & 0 \\ 0 & 0 & u_j & 0 & \frac{1}{\rho}\delta_{2j} & 0 & \dots & 0 \\ 0 & 0 & 0 & u_j & \frac{1}{\rho}\delta_{3j} & 0 & \dots & 0 \\ 0 & \rho c^2\delta_{1j} & \rho c^2\delta_{2j} & \rho c^2\delta_{2j} & u_j & 0 & \dots & 0 \\ 0 & 0 & 0 & 0 & 0 & u_j & \dots & 0 \\ \vdots & \vdots & \vdots & \vdots & \vdots & & \ddots & 0 \\ 0 & 0 & 0 & 0 & 0 & 0 & 0 & u_j \end{bmatrix}. \tag{56}$$

The wave decomposition involves computing the eigenvalues and eigenvectors, and from these the wave amplitude variations. For the sake of brevity and clarity, we will present below only the analysis pertinent to $\mathbf{A}^1$ and $\partial\phi/\partial x_1$, referring to boundary conditions across a surface of fixed $x_1$. A similar derivation is made for the other two dimensions.

Considering $\mathbf{A}^1$:

$$\mathbf{A}^1 = \begin{bmatrix} u_1 & \rho & 0 & 0 & 0 & 0 & \dots & 0 \\ 0 & u_1 & 0 & 0 & \frac{1}{\rho} & 0 & \dots & 0 \\ 0 & 0 & u_1 & 0 & 0 & 0 & \dots & 0 \\ 0 & 0 & 0 & u_1 & 0 & 0 & \dots & 0 \\ 0 & \rho c^2 & 0 & 0 & u_1 & 0 & \dots & 0 \\ 0 & 0 & 0 & 0 & 0 & u_1 & \dots & 0 \\ \vdots & \vdots & \vdots & \vdots & \vdots & \vdots & \ddots & 0 \\ 0 & 0 & 0 & 0 & 0 & 0 & 0 & u_1 \end{bmatrix}, \tag{57}$$

its eigenvalues, $\lambda_i$, are determined from

$$\det(\lambda \mathbf{I} - \mathbf{A}^1) = (\lambda - u_1)^{N+3} \left[ (\lambda - u_1)^2 - c^2 \right] = 0 \tag{58}$$

as

$$\lambda = u_1 - c, u_1, u_1, \cdots, u_1, u_1, u_1 + c. \tag{59}$$

These eigenvalues represent either the velocities of sound waves moving in the negative ($\lambda_1$) or positive ($\lambda_{N+5}$) directions along the $x_1$ axis relative to the local convection velocity, or the velocities of waves moving at the local convection velocity ($\lambda_2$ to $\lambda_{N+4}$).

Associated with these eigenvalues are the left eigenvectors $l$ of $\mathbf{A}^1$ satisfying $l \cdot \mathbf{A}^1 = \lambda l$:

$$\lambda_1 = u_1 - c : l = \begin{bmatrix} 0 & -\rho c & 0 & 0 & 1 & 0 & \cdots & 0 \end{bmatrix}, \tag{60}$$

$$\lambda_2 = u_1 : l = \begin{bmatrix} -c^2 & 0 & 0 & 0 & 1 & 0 & \cdots & 0 \end{bmatrix}, \tag{61}$$

$$\lambda_3 = u_1 : l = \begin{bmatrix} 0 & 0 & 1 & 0 & 0 & 0 & \cdots & 0 \end{bmatrix}, \tag{62}$$

$$\lambda_4 = u_1 : l = \begin{bmatrix} 0 & 0 & 0 & 1 & 0 & 0 & \cdots & 0 \end{bmatrix}, \tag{63}$$

$$\lambda_i = u_1, i = 5, N+4 : l = \begin{bmatrix} 0 & 0 & 0 & 0 & 0 & \delta_{i5} & \cdots & \delta_{iN+4} \end{bmatrix}, \tag{64}$$

$$\lambda_{N+5} = u_1 + c : l = \begin{bmatrix} 0 & \rho c & 0 & 0 & 1 & 0 & \cdots & 0 \end{bmatrix}. \tag{65}$$

The procedure is continued by computing the quantities $\mathcal{L}_i$ from $\mathcal{L}_i = \lambda_i l \partial\phi/\partial x_1 = l \cdot \mathbf{A}^1 \partial\phi/\partial x_1$:

$$\mathcal{L}_1 = (u_1 - c)\left[\frac{\partial p}{\partial x_1} - \rho c \frac{\partial u_1}{\partial x_1}\right] \text{ for } \lambda_1 = u_1 - c, \tag{66}$$

$$\mathcal{L}_2 = u_1\left[\frac{\partial p}{\partial x_1} - c^2 \frac{\partial \rho}{\partial x_1}\right] \text{ for } \lambda_2 = u_1, \tag{67}$$

$$\mathcal{L}_3 = u_1\left(\frac{\partial u_2}{\partial x_1}\right) \text{ for } \lambda_3 = u_1, \tag{68}$$

$$\mathcal{L}_4 = u_1 \left( \frac{\partial u_3}{\partial x_1} \right) \text{ for } \lambda_4 = u_1, \tag{69}$$

$$\mathcal{L}_{\alpha+4} = u_1 \left( \frac{\partial Y_\alpha}{\partial x_1} \right) \text{ for } \lambda_{\alpha+4} = u_1, \alpha = 1, N, \tag{70}$$

$$\mathcal{L}_{N+5} = (u_1 + c) \left[ \frac{\partial p}{\partial x_1} + \rho c \frac{\partial u_1}{\partial x_1} \right] \text{ for } \lambda_{N+5} = u_1 + c. \tag{71}$$

As pointed out by Poinsot and Lele [1], by consequence of their definition

$$\left( l \frac{\partial \phi}{\partial t} \right)_i = -\mathcal{L}_i,$$

and thus the $\mathcal{L}_i$ represent the time variation of the wave amplitude for each component of the vector $\phi$, each $\mathcal{L}_i$ being associated with a wave having the speed $\lambda_i$. By manipulating the $\mathcal{L}_i$ one may influence the amplitude of waves crossing a given boundary and in particular hope to suppress spurious, unphysical waves. We note that, as mentioned above, diffusive terms are not included in this analysis and neither are source/sink terms; the implicit assumption is that the ellipticity of the equations plays a secondary role in determining the character of the solution at the boundary.

### 2.3. Euler Equations Wave Decomposition

According to Poinsot and Lele [1], it is possible to find potential $\mathcal{L}_i$ values for the more general case of the complete equations (see Section 4 below) by exploring the simpler case of a LODI system of equations. These LODI relationships are only used to find constraints between the dependent variables and the wave amplitude variation at the domain boundaries.

To accomplish this analysis, the Euler equations are cast in terms of the wave amplitude variations by first calculating the spatial derivatives in terms of the $\mathcal{L}_i$:

$$\frac{\partial \rho}{\partial x_1} = \frac{1}{2c^2}\left[\frac{\mathcal{L}_{N+5}}{(u_1+c)} + \frac{\mathcal{L}_1}{(u_1-c)}\right] - \frac{\mathcal{L}_2}{u_1 c^2}, \tag{72}$$

$$\frac{\partial u_1}{\partial x_1} = \frac{1}{2\rho c}\left[\frac{\mathcal{L}_{N+5}}{(u_1+c)} - \frac{\mathcal{L}_1}{(u_1-c)}\right], \tag{73}$$

$$\frac{\partial u_2}{\partial x_1} = \frac{\mathcal{L}_3}{u_1}, \tag{74}$$

$$\frac{\partial u_3}{\partial x_1} = \frac{\mathcal{L}_4}{u_1}, \tag{75}$$

$$\frac{\partial p}{\partial x_1} = \frac{1}{2}\left[\frac{\mathcal{L}_{N+5}}{(u_1+c)} + \frac{\mathcal{L}_1}{(u_1-c)}\right], \tag{76}$$

$$\frac{\partial Y_\alpha}{\partial x_1} = \frac{\mathcal{L}_{\alpha+4}}{u_1}. \tag{77}$$

The LODI system for the primitive variables containing time- and $x_1$-derivative terms is recast in terms of the $\mathcal{L}_i$ as:

$$\frac{\partial \rho}{\partial t} + \frac{1}{c^2}\left[\frac{(\mathcal{L}_{N+5} + \mathcal{L}_1)}{2} - \mathcal{L}_2\right] = 0, \tag{78}$$

$$\frac{\partial u_1}{\partial t} + \frac{\mathcal{L}_{N+5} - \mathcal{L}_1}{2\rho c} = 0, \tag{79}$$

$$\frac{\partial u_2}{\partial t} + \mathcal{L}_3 = 0, \tag{80}$$

$$\frac{\partial u_3}{\partial t} + \mathcal{L}_4 = 0, \tag{81}$$

$$\frac{\partial p}{\partial t} + \frac{\mathcal{L}_{N+5} + \mathcal{L}_1}{2} = 0, \tag{82}$$

$$\frac{\partial Y_\alpha}{\partial t} + \mathcal{L}_{\alpha+4} = 0; \alpha = 1, N. \tag{83}$$

From the above Eqs. 78-83, one can find the conservative variables:

$$\frac{\partial \rho}{\partial t} + d_1 = 0, \tag{84}$$

$$\frac{\partial \rho u_1}{\partial t} + u_1 d_1 + \rho d_2 = 0, \tag{85}$$

$$\frac{\partial \rho u_2}{\partial t} + u_2 d_1 + \rho d_3 = 0, \tag{86}$$

$$\frac{\partial \rho u_3}{\partial t} + u_3 d_1 + \rho d_4 = 0, \tag{87}$$

$$\frac{\partial \rho E_T}{\partial t} + \left(E_T + \frac{p}{\rho}\right) d_1 + \rho u_i d_{i+1} + \sum_{\alpha=1}^{N} \rho d_{\alpha+4} \left(\frac{\partial E}{\partial Y_\alpha}\right)_{\substack{\rho,p,Y_\beta \\ \beta \neq \alpha}} + \frac{C_p}{m \alpha_v} d_{N+5} = 0, \tag{88}$$

$$\frac{\partial \rho Y_\alpha}{\partial t} + Y_\alpha d_1 + \rho d_{\alpha+4} = 0; \alpha = 1, N, \tag{89}$$

with $\left(\frac{\partial E}{\partial Y_\alpha}\right)_{\substack{\rho,p,Y_\beta \\ \beta\neq\alpha}}$ from Eq. 41 and

$$d_1 = \frac{1}{c^2}\left[\frac{(\mathcal{L}_{N+5}+\mathcal{L}_1)}{2} - \mathcal{L}_2\right] = \rho\frac{\partial u_1}{\partial x_1} + u_1\frac{\partial \rho}{\partial x_1}, \tag{90}$$

$$d_2 = \left[\frac{\mathcal{L}_{N+5}-\mathcal{L}_1}{2\rho c}\right] = u_1\frac{\partial u_1}{\partial x_1} + \frac{1}{\rho}\frac{\partial p}{\partial x_1}, \tag{91}$$

$$d_3 = \mathcal{L}_3 = u_1\frac{\partial u_2}{\partial x_1}, \tag{92}$$

$$d_4 = \mathcal{L}_4 = u_1\frac{\partial u_3}{\partial x_1}, \tag{93}$$

$$d_{\alpha+4} = \mathcal{L}_{\alpha+4} = u_1\frac{\partial Y_\alpha}{\partial x_1}, \tag{94}$$

$$d_{N+5} = \frac{\mathcal{L}_2}{c^2} = \frac{u_1}{c^2}\left[\frac{\partial p}{\partial x_1} - c^2\frac{\partial \rho}{\partial x_1}\right], \tag{95}$$

where the $d_i$ are groups of terms involving $x_1$ derivatives that must be constrained by conditions suppressing numerically spurious behavior across the $x_1$ boundary.

For a perfect gas the energy equation becomes

$$\frac{\partial \rho E_T}{\partial t} + \tfrac{1}{2}u_i u_i d_1 + \frac{c^2(d_1+d_{N+5})}{(\gamma-1)} + \rho u_i d_{i+1} + \sum_{\alpha=1}^{N}\rho d_{\alpha+4}\left(\frac{C_{p,\alpha}T}{m_\alpha} - \frac{C_p T}{m_\alpha}\right) = 0, \tag{96}$$

## 3. APPLICATION OF CHARACTERISTIC BOUNDARY CONDITIONS

In the previous section, wave decomposition was used to rewrite the time and spatial derivatives in terms of wave amplitude variations. The implementation of the method consists in determining the correct values of these wave amplitude variations according to the nature of the problem to be solved. In this process we

distinguish between the outgoing waves which carry information from the interior of the computational domain and which therefore are based on the solution of the conservation equations, and the incoming waves which carry information from the exterior of the domain to the region where the solution is sought; these incoming waves are the origin of the spurious behavior that must be mitigated.

The implementation of the method consists in calculating the amplitude variation of outgoing waves from the derivatives at the boundary, which are based on the interior points, whereas the incoming wave amplitude variations are determined from the boundary conditions. In the discussion that follows, it is assumed that waves travelling in the $x_1 > 0$ direction exit the computational domain. The definition of incoming and outgoing waves is reversed if waves entering the domain have $\lambda_i < 0$. With this convention, at a (subsonic) boundary where $0 < u_1 < c$, the outgoing wave amplitudes are computed from the interior points, whereas the incoming wave amplitude ($\mathcal{L}_1$ corresponding to $\lambda_1 = u_1 - c$) is derived from the specified boundary conditions. On the other hand, at a (subsonic) boundary where $-c < u_1 < 0$, the incoming wave amplitude variations are set to zero (meaning that there are no waves), except for those that can be derived from the specified boundary conditions, whereas the outgoing wave amplitude variation ($\mathcal{L}_{N+5}$ corresponding to $\lambda_{N+5} = u_1 + c$) is computed from the interior points.

### 3.1. Subsonic Slip-wall Boundary Conditions

At slip walls, the normal velocity is zero, i.e. $u_1 = 0$. Then, from Eq. 79, $\mathcal{L}_1 = \mathcal{L}_{N+5}$ and the remaining wave amplitude variations are determined from the interior points using Eqs. 67 - 71.

### 3.2. Subsonic Non-reflecting Outflow Boundary Conditions

As discussed in Poinsot and Lele [1], theoretically a non-reflecting condition could be imposed by setting the amplitude of incoming waves to zero, i.e. $\mathcal{L}_1 = 0$. However, this leaves the flow with no way to maintain its pressure. To mitigate this unphysical condition, the pressure at 'infinity' is imposed through $\mathcal{L}_1 = K(p - p_\infty)$ with $K = \sigma(1 - M^2)c/L$ where $\sigma$ is a constant, $M$ is the maximum Mach number in the domain and $L$ is a characteristic size of the domain. The value of $\sigma$ can be adjusted to fit the requirement of the problem and an optimal value of 0.58 has been proposed by Rudy and Strikwerda [17] and implemented by Poinsot and Lele [1] in one of their example problems.

The remaining wave amplitude variations are determined from the interior points using Eqs. 67 through 71.

### 3.3. Supersonic Outflow Boundary Conditions

In the supersonic case, all the waves are outgoing, so the wave amplitude variations are determined from the interior points using Eqs. 66 - 71.

## 4. TESTS: PROPAGATION OF ACOUSTIC WAVES

To test the implementation of the consistent boundary condition based on the characteristic wave method we consider the one-dimensional propagation of an acoustic wave in a two-dimensional domain.

The computations are performed for a supercritical two-component nitrogen-heptane flow using the Peng-Robinson EOS as in Miller et al. [18]:

$$p = \frac{R_u T}{(v - B_m)} - \frac{A_m}{(v^2 + 2vB_m - B_m^2)}, \tag{97}$$

where $A_m$ and $B_m$ are given from mixing rules as

$$A_m = \sum_\alpha \sum_\beta X_\alpha X_\beta A_{\alpha\beta}, \qquad B_m = \sum_\alpha X_\alpha B_\alpha. \tag{98}$$

The thermodynamic properties are obtained through various derivatives and functions of the Gibbs energy ($G$):

$$G(T, p, X_\alpha) = \int_v^{v_u} p(v', T, X_\alpha) dv' + pv - R_u T + \sum_\alpha X_\alpha \left[ G_\alpha^0 + R_u T \ln(X_\alpha) \right], \tag{99}$$

where the superscript 0 represents the 'low pressure' reference condition for the integration as generally used in the departure function formalism described by Prausnitz et al. [19]. Since the integral is ill defined for a zero pressure reference condition, we choose $p^0 = 1bar$ such that $v_u = R_u T/p^0$. This leads to

$$h = G - T\left(\frac{\partial G}{\partial T}\right)_{p, X_\alpha} = h^0 + pv - R_u T + K_1 \left( A_m - T\frac{\partial A_m}{\partial T} \right), \tag{100}$$

$$C_p = \left(\frac{\partial h}{\partial T}\right)_{p,X_\alpha} = C_p^0 - T\,\frac{(\partial p/\partial T)^2_{v,X_\alpha}}{(\partial p/\partial v)_{T,X_\alpha}} - R_u - T\frac{\partial^2 A_m}{\partial T^2}K_1, \tag{101}$$

where $h^0$ is the reference molar enthalpy and $C_p^0 = \partial h^0/\partial T$ is the reference molar heat capacity,

$$\left(\frac{\partial p}{\partial T}\right)_{v,X_\alpha} = \frac{R_u}{(v - B_m)} - \frac{(\partial A_m/\partial T)}{(v^2 + 2vB_m - B_m^2)}, \tag{102}$$

$$\left(\frac{\partial p}{\partial v}\right)_{T,X} = \frac{-R_u T}{(v - B_m)^2}\left[1 - 2A_m\left\{R_u T(v + B_m)\left(\frac{v}{v - B_m} + \frac{B_m}{v + B_m}\right)^2\right\}^{-1}\right], \tag{103}$$

$$K_1 = \frac{1}{2\sqrt{2}B_m}\ln\left[\frac{v + (1 - \sqrt{2})B_m}{v + (1 + \sqrt{2})B_m}\right]. \tag{104}$$

The conservation equations for the binary heptane-nitrogen mixture are those of Section 2 with heptane being species 1 and nitrogen being species 2.

All test cases below pertain to a two-dimensional domain $(x_1, x_2)$ of respective dimensions $L_1 = 0.2$ m and $L_2 = 232$ m. The initial condition specifies uniform

profiles for $u_1$ and $T$, with

$$w = a_1 \exp\left(-a_2 x_2/\delta\right); -L_2/2 \leq x_2 \leq L_2/2, \tag{105}$$

$$u_2 = u_2(x_2) = w, \tag{106}$$

$$p = p\left(x_2\right) = p_\infty(1+w), \tag{107}$$

$$Y_2 = Y_2\left(x_2\right) = 0.5 + a_3 \frac{x_2}{L_2/2}, \tag{108}$$

and the density is calculated from the EOS. These initial conditions lead to two waves, each propagating toward one boundary. We test the validity of the boundary conditions implementation by computing three subsonic ($M_\infty = 0.4$) cases with $a_1 = 0.1$, $a_2 = 5.678$, $\delta = 6.859 \times 10^{-3}$, $T = 600K$ and $p_\infty = 60$ atm. Also evaluated is the simplistic approach whereby the term $\dfrac{1}{\gamma - 1}$ is replaced by $\dfrac{\rho E + p}{\rho c^2}$ in the characteristic form of the energy equation derived from the perfect gas formulation [1], and $\mathcal{L}_5 = \mathcal{L}_6 = 0$ for the mass fractions. For each of the test cases, we compare the predictions of the simplistic approach with those of the fundamental approach derived here.

The numerical scheme in the present simulations uses fourth-order Runge-Kutta time integration and eighth-order finite-differencing, and the resolution is $50 \times 232$ points. Periodic conditions are employed in the $x_1$ direction, and subsonic non-reflecting outflow conditions are used with null mass fraction gradient in the $x_2$ direction. The viscous conditions are applied as recommended by Poinsot and Lele [1]: for the subsonic outflow, the gradients of the heat flux and of the shear stresses normal to the boundary are set to zero.

**Test 1**: The first case has an initially uniform condition for the mass fraction ($a_3 = 0$) with $u_1$ =145 m/s. Figure 1 shows the density and pressure before the waves reach the boundaries ($N_{time}$ is the number of time steps), whereas Fig. 2 shows them after the wave has reached the boundaries. As displayed in the figures, both $\rho$ and $p$ remain constant, as expected; the small high frequency oscillations can be attributed to the high-order (eighth-order) finite-differencing. We note, however, that the fundamental characteristic condition derived herein shows minimal reflection, in contrast to the simplistic approach result where the reflected waves can clearly be discerned.

**Test 2:** The second case has an initially linear mass fraction ($a_3 = 0.2$) with $u_1$ =137 m/s. The results are depicted in Figs. 3 and 4 where it is clear that the results are similar to Test 1: minimal reflection is obtained using the fundamental approach whereas there are spurious reflections in the simplistic approach. The $\rho$ profile remains linear at these early times because the diffusional characteristic time is considerably larger than the times at which the solution is illustrated. The acoustic time scale is $t_a = 0.5L_2/a_s \simeq 3.2 \times 10^{-4}$ s whereas the diffusional time scale estimated from the centerline values of the solution is $t_D = 0.5L_2/[\rho D\ \alpha_D\ (\partial Y_h/\partial x_2)] \simeq 0.531$ s.

**Test 3:** The third case has the same initial condition as the first, but has a time-varying mass fraction resulting from a finite heptane mass source term having a Gaussian profile. This mass source is intended to mimic features of mass sources that would arise from chemical reactions or the mass emission (not necessarily evaporation, since at supercritical conditions there is only a single phase) from chunks of supercritical fluid (usually modeled as droplets) in a spray. Due to this hep-

tane mass source term, the mass fraction is increasing with time as shown in Fig. 5 where the two lines plotted correspond to the time stations of the density and pressure profiles illustrated in Figs. 6 and 7. As in Tests 1 and 2, the fundamental compatibility conditions based on the characteristic wave analysis allow the waves to exit the boundary, whereas the simplistic approach exhibits significant reflection. Just as important, but different from Tests 1 and 2, the density and pressure profiles from the two boundary conditions do not overlap before the waves reach the boundary. The discrepancy is particularly notable at the boundary, where the density profile computed using the fundamental approach relaxes smoothly but the simplistic approach leads to a sharply increasing gradient. These results show that for multicomponent fluids the nature of the solution is affected by the simplistic approach not only at the boundaries, but also in the entire domain.

## 5. CONCLUSIONS

Consistent boundary conditions based on characteristic wave analysis were here derived for multicomponent flows governed by real gas equations of state. The governing equations account not only for departures from the perfect gas equation of state, but also for mixture non-ideality and for thermal diffusion effects. The characteristic wave analysis is based on the inherent assumption that the elliptic terms act only as corrections to the essentially hyperbolic operator. Thus, diffusional terms are not part of the consistent boundary condition analysis, but are used in the governing equations once a solution is sought. It has been pointed out that, based on the results of a diagonalization of the species and energy equations operators, the condition of weak ellipticity, which underlines this analysis, may

not always be satisfied when thermal diffusion effects are important. Whether this condition is satisfied depends on the $(p, T, Y_\alpha)$ regime and on the species under consideration, determining the value of the effective thermal conductivity.

The conditions derived herein have been tested on the one-dimensional propagation of acoustic waves in a two-dimensional domain by using subsonic non-reflecting boundaries for a binary nitrogen-heptane mixture at 600 K and 60 atm. Moreover, boundary conditions derived by simplistically replacing the gas constant in the results of Baum et al. [7] with its equivalent real gas quantities have also been tested. It is shown that whereas using the fundamental analysis results in the acoustic waves properly passing through the boundaries without reflections, the use of the simplistic approach yields significant reflections at the boundaries. Most discrepancies occurred when a source term was added to the mass fraction equations; in this case, additional to the reflections at the boundaries, the solution within the entire domain was affected by the simplistic approach, exhibiting differences from that found using the fundamental approach.

## 6. APPENDIX A: DERIVATION OF THE COMPATIBILITY CONDITIONS USING THE TEMPERATURE AS A VARIABLE

A mathematical development similar to that of Baum et al. [7] is given here for readers who find that in their application the natural primitive variable is $T$ rather than $p$. The basic equations in conservative form are

$$\frac{\partial \widetilde{U}}{\partial t} + \frac{\partial F_j}{\partial x_j} + \widetilde{C} = 0$$

where

$$\widetilde{U} = (\rho, \rho E_T, \rho u_i, \rho Y_\alpha) \quad (i \in [1,3], \alpha \in [1,N]),$$

$$F_j = [\rho u_j, (\rho E_T + p)u_j, \rho u_i u_j + p\delta_{ij}, \rho Y_\alpha u_j],$$

$$\widetilde{C} = [-S_I, \nabla \cdot \overrightarrow{q}_{IK} - \frac{\partial(u_i \tau_{ij})}{\partial x_j} - S_{III}, -\frac{\partial \tau_{ij}}{\partial x_j} - S_{II,i}, \nabla \cdot \overrightarrow{J}_\alpha - S_{I,\alpha}],$$

where the $S$'s are source terms (e.g. Miller and Bellan [20]) with $S_I = \sum_\alpha S_{I,\alpha}$. As in Baum et al. [7] and above, the characteristic form of the equations is obtained from their primitive form

$$\frac{\partial U}{\partial t} + \mathbf{A}^j \cdot \frac{\partial U}{\partial x_j} + C = 0$$

where

$$U = (\rho, T, u_i, Y_\alpha),$$

and $\mathbf{A}^j = \mathbf{P}^{-1} \cdot \mathbf{Q}_j$, $C = \mathbf{P}^{-1} \cdot \widetilde{C}$ where $\mathbf{P} \equiv \partial \widetilde{U}/\partial U$ and $\mathbf{Q}_j \equiv \partial F_j/\partial U$. The matrix $\mathbf{P}$ has the same form as in Baum et al. [7] with the diagonal elements equal

to $\rho$ and all other elements null except

$$P_{1,1} = 1,$$

$$P_{2,m} = \rho u_{m-2} \quad \text{for } m \in [3,5],$$

$$P_{m,1} = u_{m-2} \quad \text{for } m \in [3,5],$$

$$P_{5+\alpha,1} = Y_\alpha,$$

and differing from Baum et al. [7]

$$P_{2,1} = H + \frac{1}{2}u_i u_i - \frac{\alpha_v T}{\rho \kappa_T},$$

$$P_{2,2} = \frac{C_v}{v} = \frac{C_p}{v} - \frac{\alpha_v^2 T}{\kappa_T},$$

$$P_{2,5+\alpha} = \rho(H_\alpha - \frac{\alpha_v T}{\kappa_T}\frac{v_\alpha}{m_\alpha})$$

where $H_\alpha = \partial H/\partial Y_\alpha$. The resulting $\mathbf{A}^j$ has $u_j$ as its diagonal elements, with other elements being null, except

$$A^j_{1,m} = \rho\delta_{m-2,j}, \quad m \in [3,5],$$

$$A^j_{2,m} = \omega_1\delta_{m-2,j}, \quad m \in [3,5],$$

$$A^j_{n,m} = \omega_{m+1}\delta_{n-2,j}, \quad m = 1,2 \text{ and } n \in [3,5]$$

$$A^j_{n,m} = \frac{p_{,\alpha}}{\rho}\delta_{n-2,j}, \quad m = \alpha + 5 \text{ and } n \in [3,5]$$

with

$$\omega_1 \equiv \frac{\alpha_v T v}{C_v \kappa_T}, \quad \omega_2 \equiv \frac{1}{\rho^2 \kappa_T}, \quad \omega_3 \equiv \frac{\alpha_v}{\rho\kappa_T}, \quad p_{,\alpha} \equiv \frac{\rho}{\kappa_T}\frac{v_\alpha}{m_\alpha}.$$

We note that for a perfect gas, matrices $\mathbf{P}$ and $\mathbf{A}^j$ coincide with those obtained by Baum et al. [7]. Following the derivation of Baum et al. [7] for the boundary whose normal is in the $j = 1$ direction, we calculate the eigenvalues of $\mathbf{A}^1$. However, for notational convenience, here we order the eigenvalues differently so as to obtain a

more compact notation when specifying the vector and matrix elements

$$\lambda = (u_1 + c, u_1 - c, u_1, u_1, u_1, u_1, ....) = (\lambda_m).$$

The first two eigenvalues correspond to the acoustic modes, the third to the entropy mode, the fourth and fifth to the transverse velocities $u_2$ and $u_3$, and finally the last $\alpha$ last ones correspond to the mass fraction modes. Corresponding to the eigenvalues, left eigenvectors are used as rows of a matrix $\mathbf{S}^1$, while $(\mathbf{S}^1)^{-1}$ has as its columns the right eigenvectors of $\mathbf{A}^1$. The elements of $(\mathbf{S}^1)^{-1}$ are $(S^1)^{-1}_{ij} = \delta_{ij}$ except

$$(S^1)^{-1}_{1,1} = (S^1)^{-1}_{1,2} = \frac{1}{2c^2}, \quad (S^1)^{-1}_{2,1} = (S^1)^{-1}_{2,2} = \frac{\alpha_v T v}{2C_p},$$

$$(S^1)^{-1}_{1,3} = -\frac{1}{c^2}, \quad (S^1)^{-1}_{2,3} = \frac{\kappa_s}{\alpha_v}, \quad (S^1)^{-1}_{3,1} = -(S^1)^{-1}_{3,2} = \frac{1}{2\rho c},$$

$$(S^1)^{-1}_{2,\alpha+5} = -\frac{\rho}{\alpha_v}\frac{v_\alpha}{m_\alpha}, \quad (S^1)^{-1}_{3,3} = 0.$$

The mode amplitude variations are defined using the left eigenvectors through

$$\mathcal{L} = \mathbf{S}^1 \cdot \mathbf{A}^1 \cdot \partial U / \partial x_1$$

and the corresponding terms in the conservative form of the equations are

$$\widetilde{\mathcal{L}} = \mathbf{M}^1 \cdot \mathcal{L}$$

where $\mathbf{M}^1 \equiv \mathbf{P} \cdot (\mathbf{S}^1)^{-1}$. The explicit expressions for $\mathcal{L}$ and $\widetilde{\mathcal{L}}$ are:

$$\mathcal{L}_1 = (u_1 + c)\left[\frac{\partial p}{\partial x_1} + \rho c \frac{\partial u_1}{\partial x_1}\right],$$

$$\mathcal{L}_2 = (u_1 - c)\left[\frac{\partial p}{\partial x_1} - \rho c \frac{\partial u_1}{\partial x_1}\right],$$

$$\mathcal{L}_3 = u_1\left[\frac{\partial p}{\partial x_1} - c^2 \frac{\partial \rho}{\partial x_1}\right],$$

$$\mathcal{L}_4 = u_1\left(\frac{\partial u_2}{\partial x_1}\right),$$

$$\mathcal{L}_5 = u_1\left(\frac{\partial u_3}{\partial x_1}\right),$$

$$\mathcal{L}_{\alpha+5} = u_1\left(\frac{\partial Y_\alpha}{\partial x_1}\right),$$

and

$$\widetilde{\mathcal{L}}_1 = \frac{\partial(\rho u_1)}{\partial x_1} = \frac{\frac{1}{2}\mathcal{L}_1 + \frac{1}{2}\mathcal{L}_2 - \mathcal{L}_3}{c^2},$$

$$\widetilde{\mathcal{L}}_2 = \frac{\partial(\rho u_1 H_T)}{\partial x_1} = \sum_{i=1}^{3} M^1_{2,i}\mathcal{L}_i + \rho(u_2\mathcal{L}_4 + u_3\mathcal{L}_5 + \sum_{\alpha}\widetilde{E}_\alpha\mathcal{L}_\alpha),$$

$$\widetilde{\mathcal{L}}_3 = \frac{\partial(p + \rho u_1^2)}{\partial x_1} = \frac{1}{c}\left[\frac{1}{2}(\frac{u_1}{c} + 1)\mathcal{L}_1 + \frac{1}{2}(\frac{u_1}{c} - 1)\mathcal{L}_2 - \frac{u_1}{c}\mathcal{L}_3\right],$$

$$\widetilde{\mathcal{L}}_4 = \frac{\partial(\rho u_1 u_2)}{\partial x_1} = \frac{u_2}{c^2}(\frac{1}{2}\mathcal{L}_1 + \frac{1}{2}\mathcal{L}_2 - \mathcal{L}_3) + \rho\mathcal{L}_4,$$

$$\widetilde{\mathcal{L}}_5 = \frac{\partial(\rho u_1 u_3)}{\partial x_1} = \frac{u_3}{c^2}(\frac{1}{2}\mathcal{L}_1 + \frac{1}{2}\mathcal{L}_2 - \mathcal{L}_3) + \rho\mathcal{L}_5,$$

$$\widetilde{\mathcal{L}}_{\alpha+5} = \frac{\partial(\rho u_1 Y_\alpha)}{\partial x_1} = \frac{Y_\alpha}{c^2}(\frac{1}{2}\mathcal{L}_1 + \frac{1}{2}\mathcal{L}_2 - \mathcal{L}_3) + \rho\mathcal{L}_{\alpha+5},$$

where

$$\frac{\partial p}{\partial x_1} = \frac{\alpha_v}{\kappa_T}\frac{\partial T}{\partial x_1} + \frac{1}{\rho\kappa_T}\frac{\partial \rho}{\partial x_1} + \frac{\rho}{\kappa_T}\sum_{\alpha}\frac{v_\alpha}{m_\alpha}\frac{\partial Y_\alpha}{\partial x_1}$$

$$H_T \equiv H + \frac{1}{2} u_i u_i,$$

$$M^1_{2,1} = \frac{1}{2}\left(\frac{H_T}{c^2} + \frac{u_1}{c}\right),$$

$$M^1_{2,2} = \frac{1}{2}\left(\frac{H_T}{c^2} - \frac{u_1}{c}\right),$$

$$M^1_{2,3} = \frac{1}{c^2}\left(\frac{C_p}{m\alpha_v} - H_T\right),$$

$$\widetilde{E}_\alpha = H_\alpha - \frac{C_p}{v\alpha_v}\frac{v_\alpha}{m_\alpha}.$$

These relationships which are valid for real gases and non-ideal mixtures are equivalent to those of Baum et al. [7] which were derived for perfect gases and ideal mixtures only.

ACKNOWLEDGMENT

This study was conducted at the Jet Propulsion Laboratory (JPL) and sponsored jointly by the Air Force Office of Scientific Research under the direction of Dr. Julian Tishkoff and by the Army Research Office under the direction of Dr. David Mann under an interagency agreement with the National Aeronautics and Space Administration. The computational resources were provided by the JPL Supercomputing Center.

## REFERENCES


1. T. J. Poinsot and S. K. Lele, Boundary conditions for direct simulations of compressible viscous flows, *J. Comp. Phys.* **101**, 104 (1992).

2. P. Dutt, Stable boundary conditions and difference schemes for Navier-Stokes equations, *SIAM J. Numer. Anal.* **25**(2), 245 (1988).

3. H.-O. Kreiss, Initial boundary value problems for hyperbolic systems, *Commun. Pure Appl. Math.* **23**, 277 (1970).

4. B. Engquist and A. Majda, Absorbing boundary-conditions for numerical-simulation of waves, *Math. Comput.* **31**(139), 629 (1977).

5. R. L. Higdon, Initial-boundary value problems for linear hyperbolic systems, *SIAM Rev.* **28**(2), 177 (1986).

6. K. Thompson, Time dependent boundary conditions for hyperbolic systems, *J. Comp. Phys.* **68**, 1 (1987).

7. M. Baum, T. Poinsot, and D. Thévenin, Accurate boundary conditions for multicomponent reactive flows, *J. Comp. Phys.* **116**, 247 (1994).

8. B. Gustafsson and A. Sundström, Incompletely parabolic problems in fluid dynamics, *SIAM J. Appl. Math.* **35**(2), 343 (1978).

9. K.-M. Shyue, A fluid-mixture type algorithm for compressible multicomponent flow with van der Waals equation of state, *J. Comp. Phys.* **156**, 43 (1999).

10. K. Harstad and J. Bellan, Isolated fluid oxygen drop behavior in fluid hydrogen at rocket chamber pressures, *Int. J. Heat Mass Transfer* **41**, 3537 (1998).

11. K. Harstad and J. Bellan, A validated all-pressure fluid drop model for binary mixtures: heptane in nitrogen, AIAA 99-206, Joint AIAA/ASME/SAE Propulsion Meeting (1999).

12. K. Harstad and J. Bellan, An all-pressure fluid drop model applied to a binary mixture: heptane in nitrogen, in press *Int. J. of Multiphase Flow* (1999).

13. S. Sarman and D. J. Evans, Heat flux and mass diffusion in binary Lennard-Jones mixtures, *Phys. Rev.* **A45**(4), 2370 (1992).

14. J. Keizer, *Statistical thermodynamics of nonequilibrium processes* (Springler-Verlag, New York, 1987).

15. R. B. Bird, W. E. Stewart and E. N. Lightfoot, *Transport Phenomena* (John Wiley and Sons, 1960).

16. K. Harstad and J. Bellan, The Lewis number under supercritical conditions, *Int. J. Heat Mass Transfer* **42**, 961 (1999).

17. D. H. Rudy and J. C. Strikwerda, A nonreflecting outflow boundary-conditions for subsonic Navier-Stokes calculations, *J. Comp. Phys.* **36(1)**, 55 (1980).

18. R. S. Miller, K. Harstad, and J. Bellan, Direct numerical simulations of supercritical fluid mixing layers applied to heptane-nitrogen, submitted to *J. Fluid Mech.* (1999).

19. J. Prausnitz, R. Lichtenthaler and E. de Azevedo, *Molecular thermodynamics for fluid-phase equilibrium* (Prentice -Hall, Inc., 1986).

20. R. S. Miller, and J. Bellan, Direct numerical simulation of a confined three-dimensional gas mixing layer with one evaporating hydrocarbon-droplet-laden stream, *J. Fluid Mech.* **384**, 293-338 (1999)

**FIG. 1.** Wave profile before reaching boundary, uniform mass fraction, $t = 2.85 \times 10^{-4}s, N_{time} = 141$

**FIG. 2.** Wave Profile after reaching boundary, uniform mass fraction, $t = 3.80 \times 10^{-4}s, N_{time} = 187$

**FIG. 3.** Wave profile before reaching boundary, linear mass fraction, $t = 2.01 \times 10^{-4}s, N_{time} = 104$

**FIG. 4.** Wave profile after reaching boundary, linear mass fraction, $t = 4.03 \times 10^{-4}s, N_{time} = 209$

**FIG. 5.** Mass fraction from heptane mass source

**FIG. 6.** Wave profile before reaching boundary, heptane mass source, $t = 2.84 \times 10^{-4}s, N_{time} = 137$

**FIG. 7.** Wave profile after reaching boundary, heptane mass source, $t = 3.80 \times 10^{-4}s, N_{time} = 182$

FIGURE 1

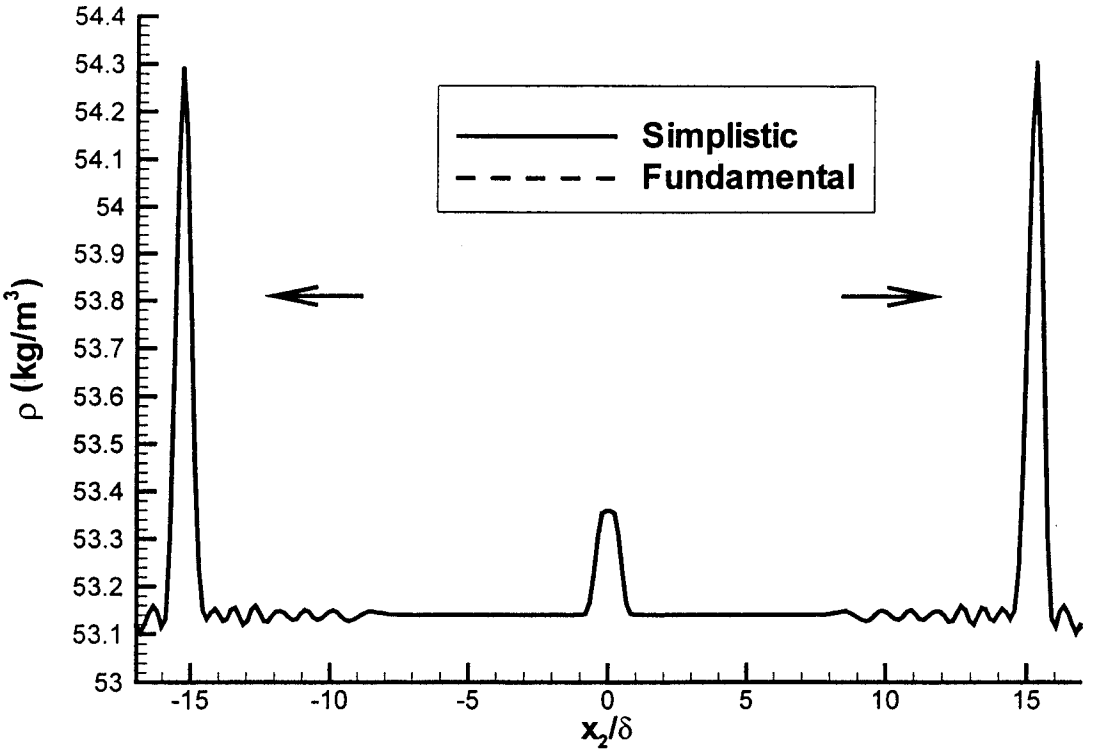
Simplistic
Fundamental
ρ (kg/m³)
54.4
54.3
54.2
54.1
54
53.9
53.8
53.7
53.6
53.5
53.4
53.3
53.2
53.1
53
-15
-10
-5
0
5
10
15
x₂/δ

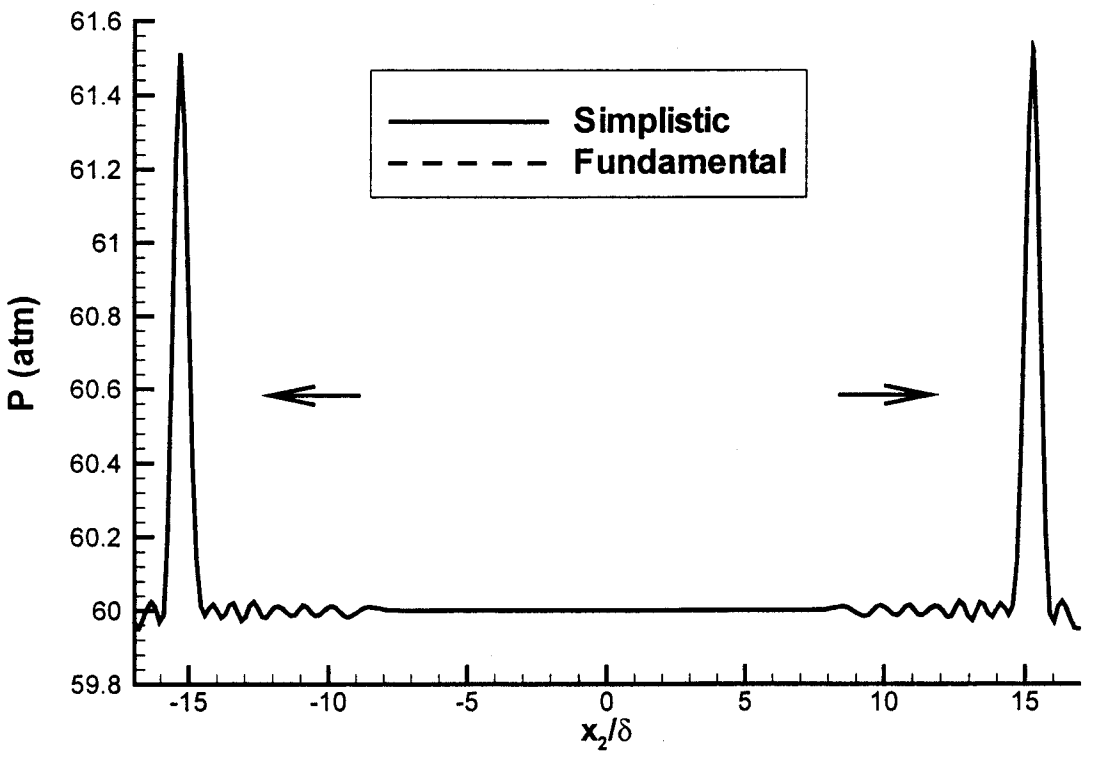
Simplistic
Fundamental
P (atm)
61.6
61.4
61.2
61
60.8
60.6
60.4
60.2
60
59.8
-15
-10
-5
0
5
10
15
x₂/δ

FIGURE 2

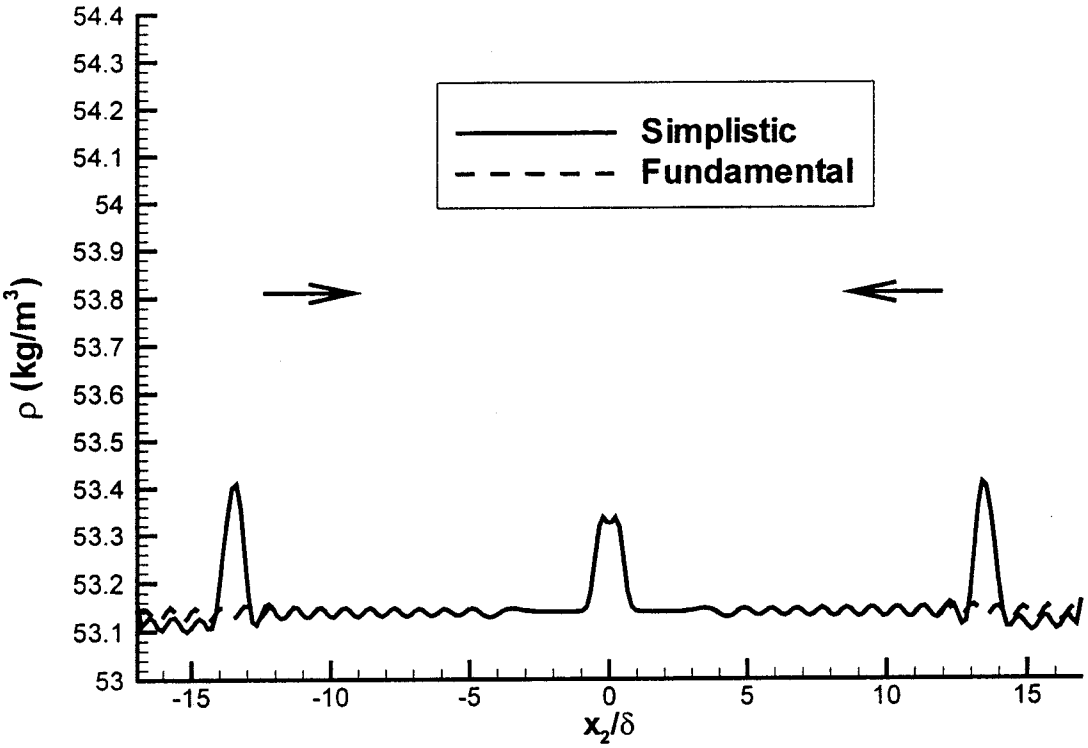
Simplistic
Fundamental
ρ (kg/m³)
54.4
54.3
54.2
54.1
54
53.9
53.8
53.7
53.6
53.5
53.4
53.3
53.2
53.1
53
-15
-10
-5
0
5
10
15
x₂/δ

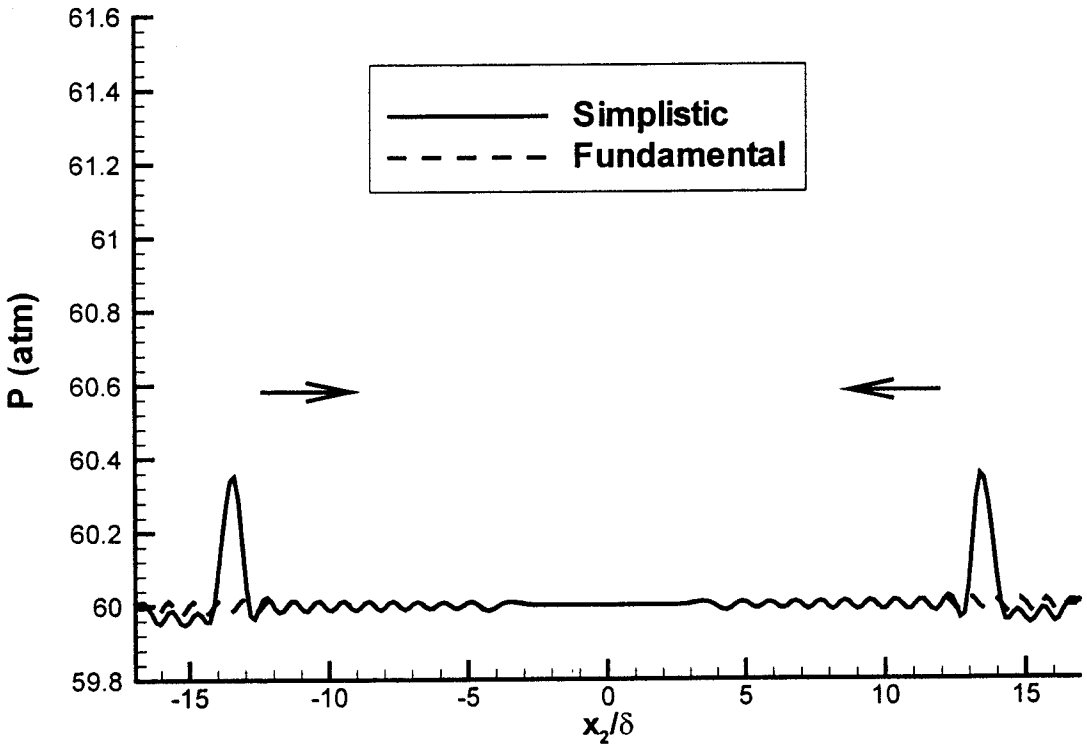
Simplistic
Fundamental
P (atm)
61.6
61.4
61.2
61
60.8
60.6
60.4
60.2
60
59.8
-15
-10
-5
0
5
10
15
x₂/δ

FIGURE 3

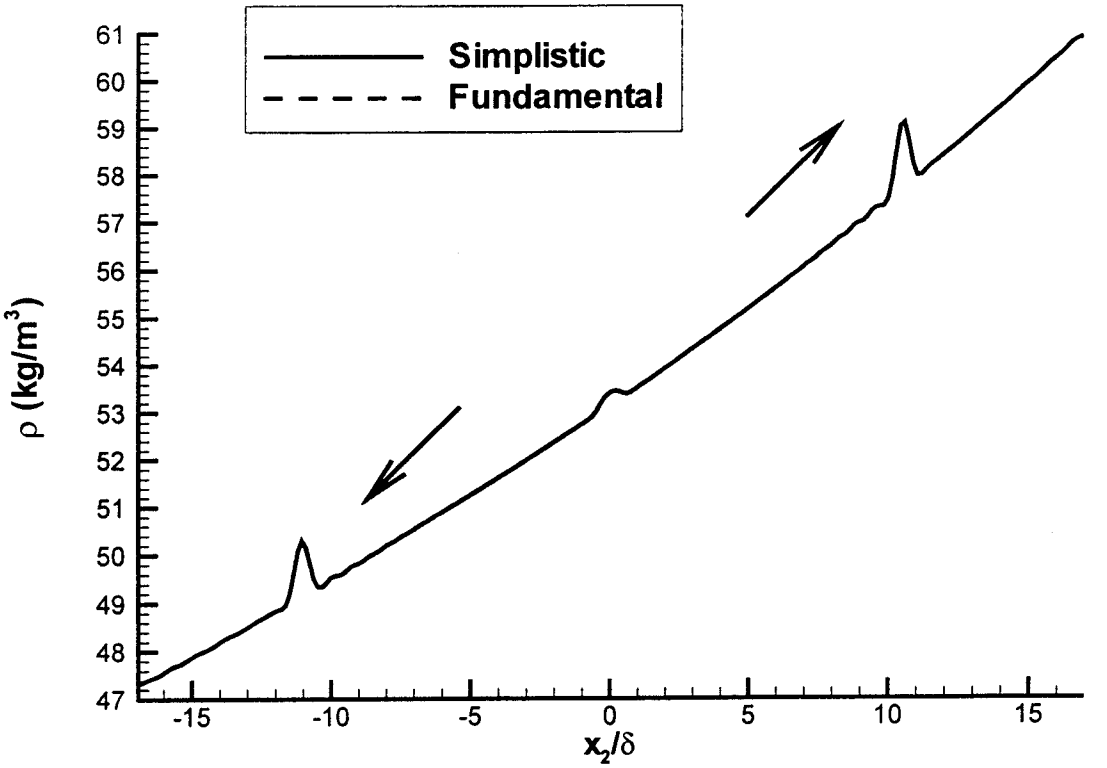
Simplistic
Fundamental
ρ (kg/m³)
61
60
59
58
57
56
55
54
53
52
51
50
49
48
47
-15
-10
-5
0
5
10
15
x₂/δ

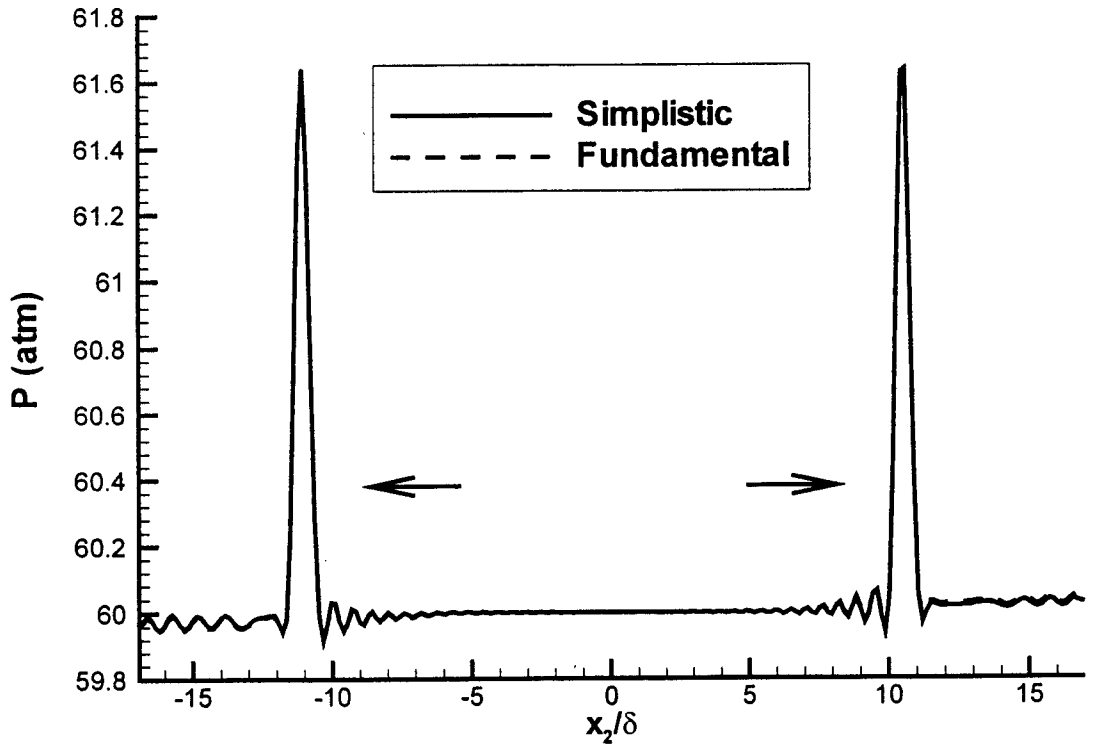
Simplistic
Fundamental
P (atm)
61.8
61.6
61.4
61.2
61
60.8
60.6
60.4
60.2
60
59.8
-15
-10
-5
0
5
10
15
x₂/δ

FIGURE 4

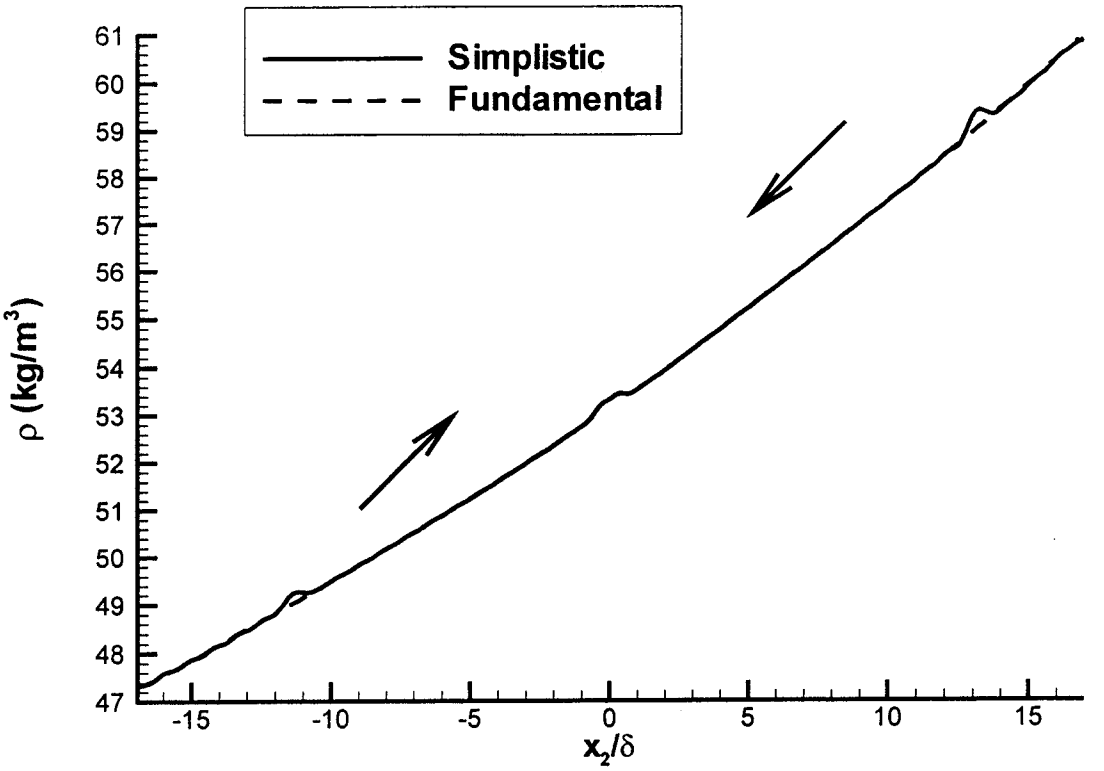
Simplistic
Fundamental
ρ (kg/m³)
61
60
59
58
57
56
55
54
53
52
51
50
49
48
47
-15
-10
-5
0
5
10
15
x₂/δ

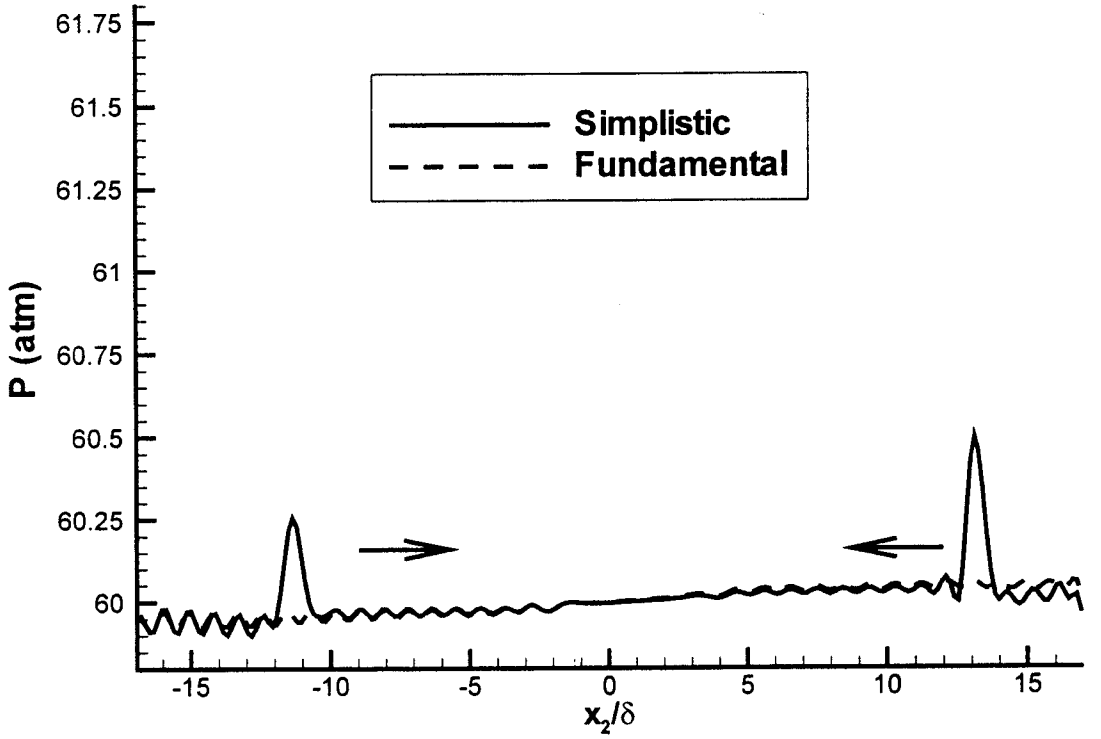
Simplistic
Fundamental
P (atm)
61.75
61.5
61.25
61
60.75
60.5
60.25
60
-15
-10
-5
0
5
10
15
x₂/δ

FIGURE 5

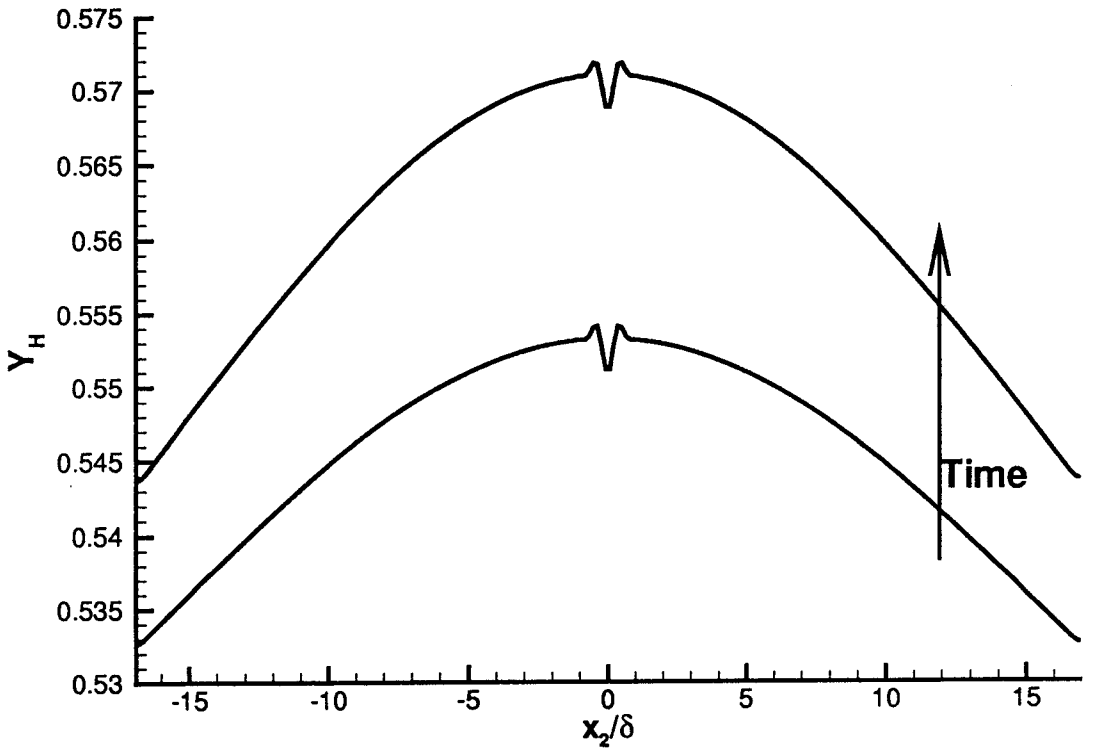
0.575
0.57
0.565
0.56
0.555
0.55
0.545
0.54
0.535
0.53
$Y_H$
-15
-10
-5
0
5
10
15
$x_2/\delta$
Time

FIGURE 6

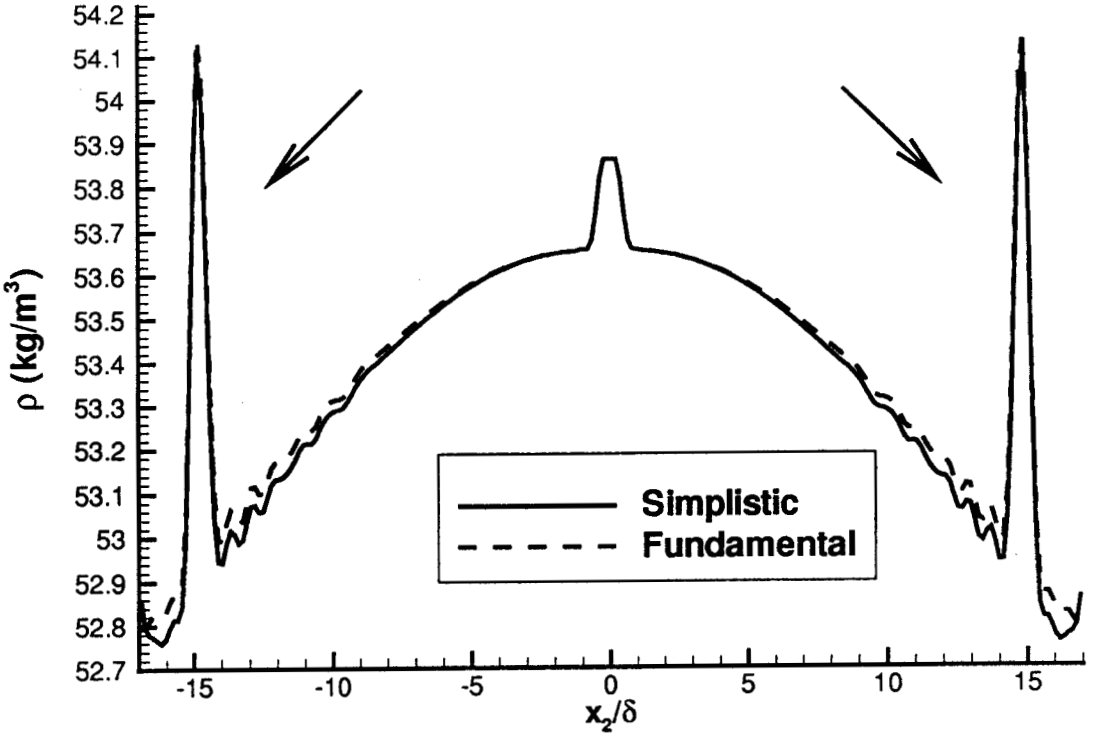
54.2
54.1
54
53.9
53.8
53.7
53.6
53.5
53.4
53.3
53.2
53.1
53
52.9
52.8
52.7
ρ (kg/m³)
-15
-10
-5
0
5
10
15
x₂/δ
Simplistic
Fundamental

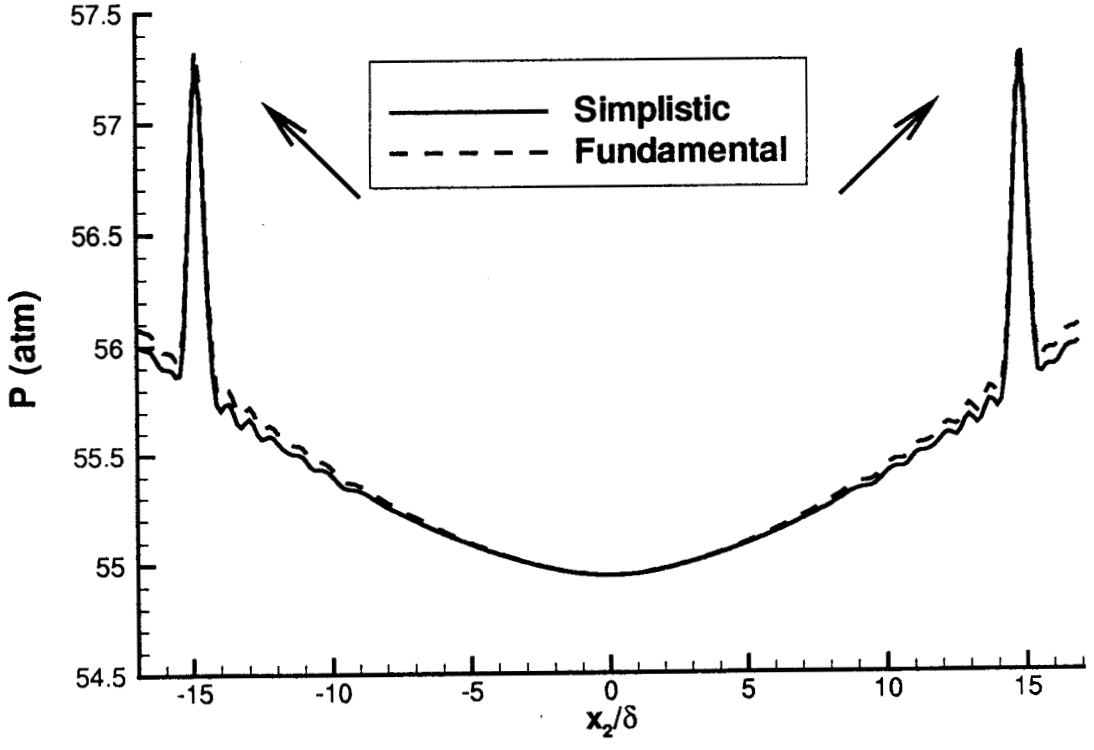
57.5
57
56.5
56
55.5
55
54.5
P (atm)
-15
-10
-5
0
5
10
15
x₂/δ
Simplistic
Fundamental

FIGURE 7

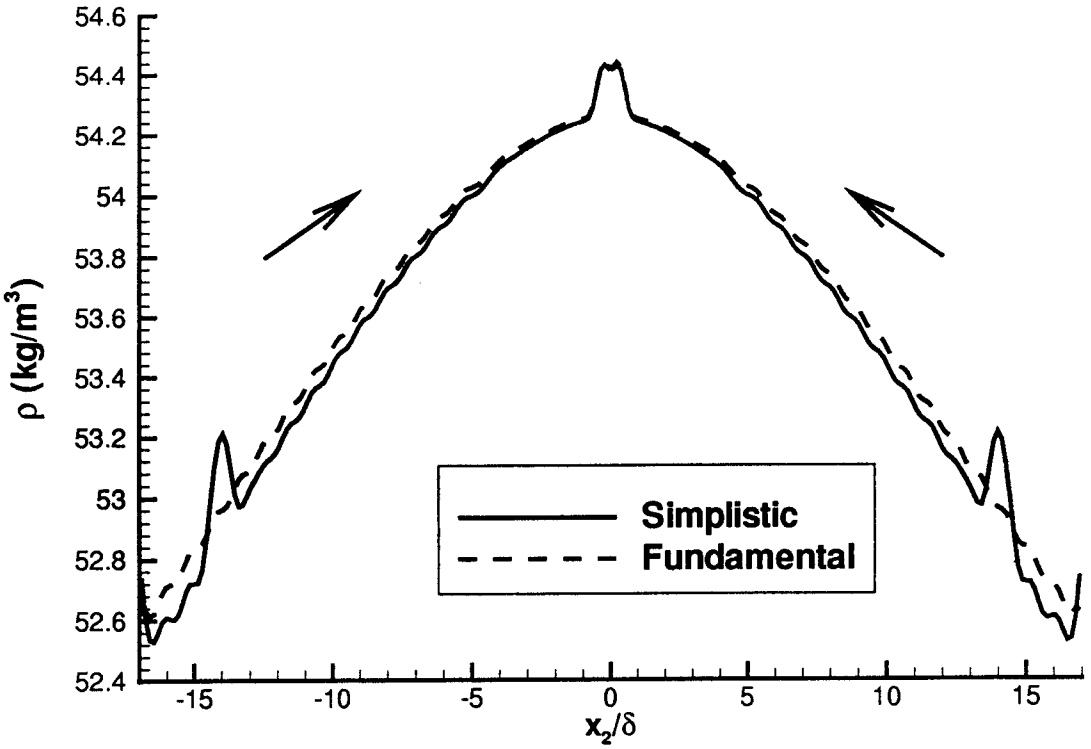
54.6
54.4
54.2
54
53.8
53.6
53.4
53.2
53
52.8
52.6
52.4
ρ (kg/m³)
-15
-10
-5
0
5
10
15
x₂/δ
Simplistic
Fundamental

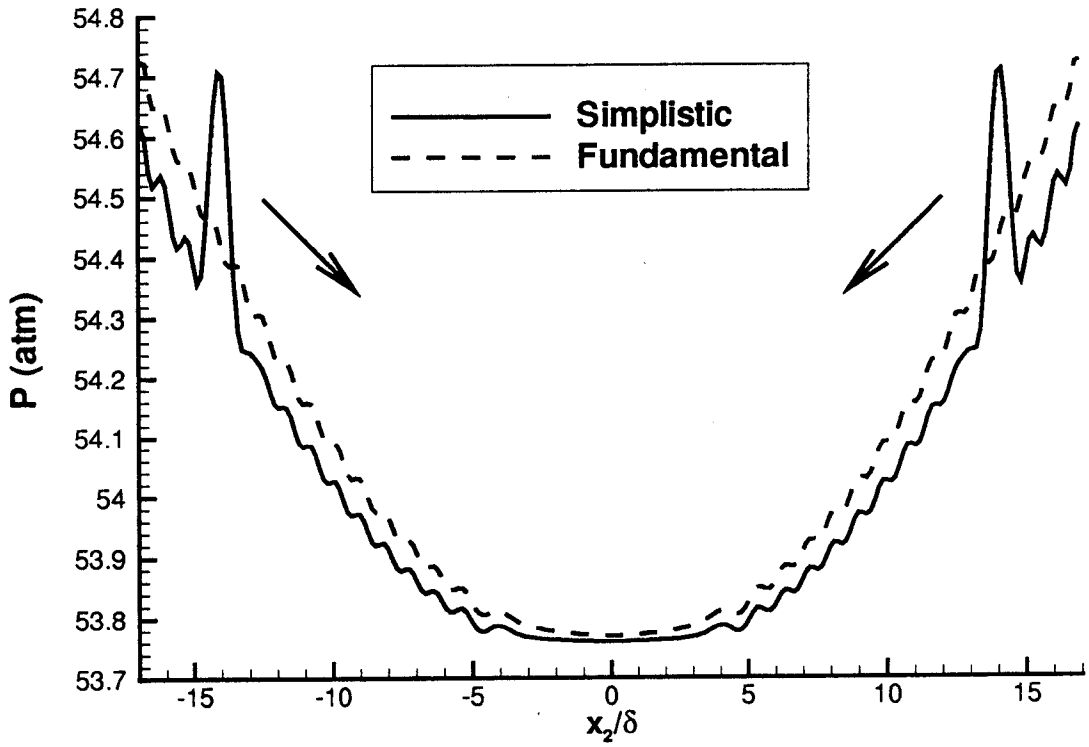
54.8
54.7
54.6
54.5
54.4
54.3
54.2
54.1
54
53.9
53.8
53.7
P (atm)
-15
-10
-5
0
5
10
15
x₂/δ
Simplistic
Fundamental